Geometric Characterisation of Light Weight Composites Using Computer Tomographic Images

Michael GODEHARDT, Katja SCHLADITZ,
Fraunhofer-Institute for Industrial Mathematics, Kaiserslautern, Germany

Abstract. One way of generating light weight composites is to insert porous ceramic grains into the melt of the matrix. The foam like inner structure of the grains causes a considerable weight reduction. On the other hand, it is desired that the mechanical properties of the matrix carry over to the composite.
The properties of the composite depend both on the structure of grains as well as on their distribution within the matrix. Therefore, computer tomographic images on two scales are used to analyse the microstructure of the grains as well as the composites.
In this paper, we describe the segmentation of the grains and analysis of their distribution in the matrix as well as segmentation and geometric characterisation of the pore structure of the grains. Connections to mechanical properties are discussed.

Introduction

Syntactic foams are generated by inserting ceramic grains into a metal or polymer melt. The foam like inner structure of the grains yields a considerable weight reduction compared to the solid matrix material. On the other hand, desired mechanical properties of the matrix like compression stress carry over to the composite. The resulting cellular composite has even better mechanical properties than conventional cellular solids made of the matrix material with equal specific weight [1].

Due to low specific weight, even foam structure which can be reproduced very well, good shaping possibilities, and convenient energy absorptivity, syntactic foams offer particular advantages for lightweight construction. In particular for sandwich constructions, the composite can be applied as core material, providing good stiffness and strength properties. The high energy absorptivity additionally promises good application possibilities as crash absorbers. Low material costs are a further advantage due to the use of recycled glass for the production of the mineral foam grains.

In order to apply syntactic foams on a large scale, insight into the resulting microstructure as well as a better understanding of the relations between microstructure and material properties is needed. To this end, both the microstructure of the composite and the pore structure of the grains have to be examined. Figure 1 gives an impression of a syntactic foam and the grains on the macroscopic scale.

For the mineral foam grains, the internal pore structure (sizes and shapes) and the state of the grain wall are the most important characteristics. In order to measure features of individual pores like volume or shape factors, they have to be separated using image processing tools as the cell walls are not conserved completely. Moreover, apertures in the cell walls are observed surprisingly frequently. For the composite, the distribution of the thicknesses of the walls between the grains was investigated.

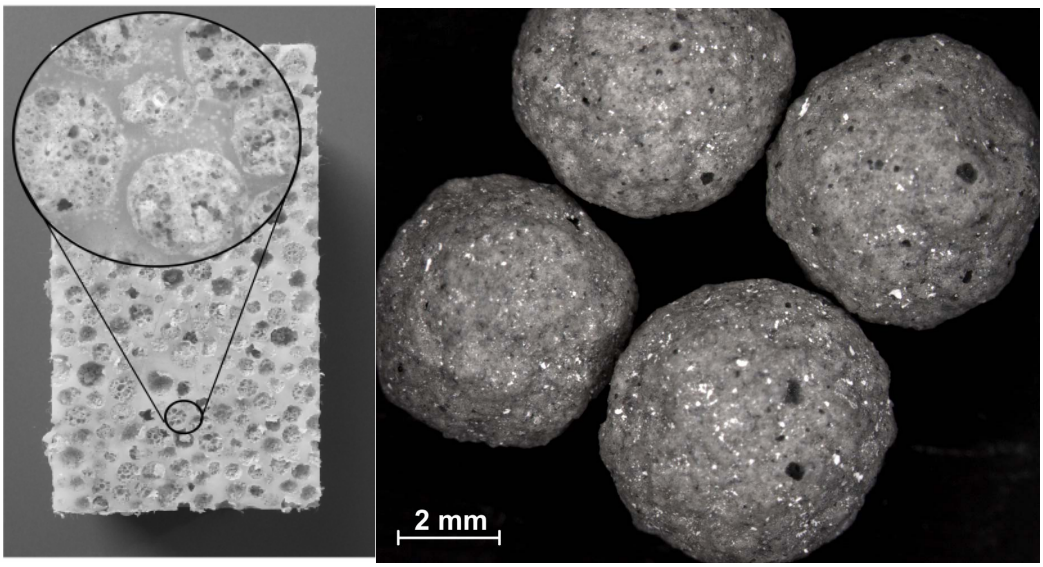

Figure 1. Syntactic foam with a polymer matrix (left) and ceramic grains (right) [1].

1. Microstructure of Light Weight Composites

1.1 Segmentation of the Ceramic Grains

First, the reconstructed tomographic image has to be presegmented. This includes preprocessing like noise removal or contrast enhancement as well as segmentation of the grey value image into a binary image of the grains as foreground and the matrix as background. Due to the close packing of the grains in the syntactic foam, some grains in the binary image are touching each other. For proper analysis these cells have to be separated and the broken facets of these cells have to be closed. This is achieved using the watershed transformation on the distance image of the presegmented image (see e. g. [2, 3]):

The Euclidean distance transformation [4] yields an image whose grey values are the distances of the respective pixels to the next pixel in the matrix. If the grains were exactly ball shaped, the local maxima in this distance image were the grain centres. Inversion of the distance image turns the local maxima into minima. Now *the watershed transformation* [5] separates the touching grains: The grey values are interpreted as topographic heights and each local minimum is a water source. Water rises from the lowest grey values. Each time waters from different sources meet, a watershed is erected. Finally, the image is completely divided into basins, one for each local minimum. Masking with the binary image of the grains then yields the separated grains.

However, digitisation effects, deviation of the grain shape from ideal balls, and noise cause additional local maxima in the distance image not being grain centres. These superfluous local maxima have to be removed before applying the watershed transformation. A particularly suitable filter is *the morphological h-maxima transform* [6], which removes local maxima if their relative height compared to neighbouring local maxima is below a certain threshold while preserving shapes and relative distance values, see Figure 5 (left).

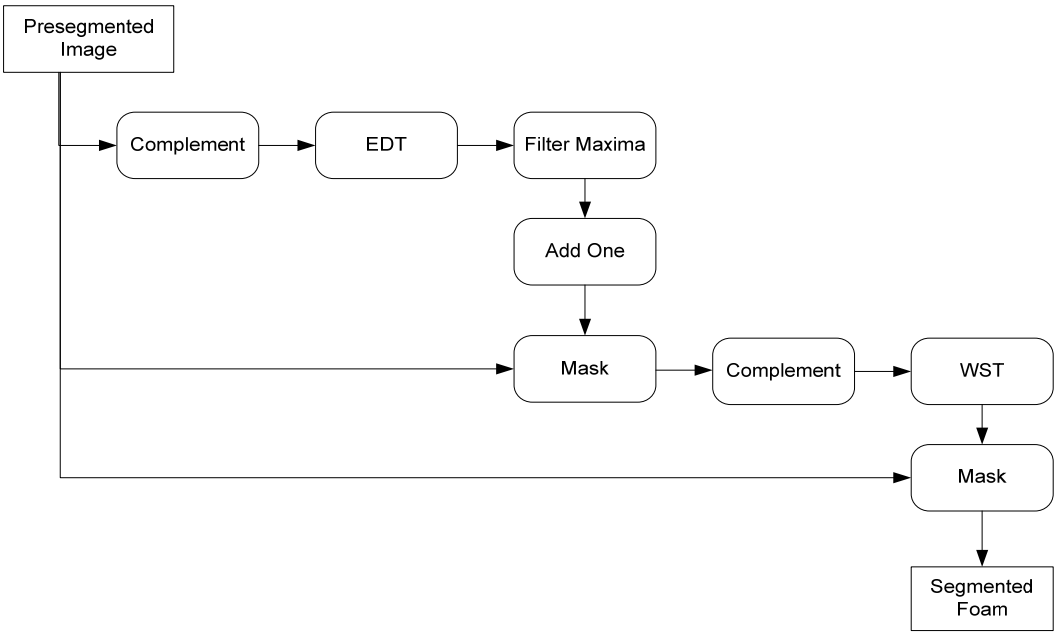

Figure 2. Processing chain for segmentation of the grains in the syntactic foam (EDT: Euclidean Distance Transformation, WST: Watershed Transformation).

Filtering the distance image yields non-zero grey values also in regions belonging to the matrix. Therefore, the matrix has to be restored by masking. Raising by one grey value ensures that the matrix regions are the lowest. Figure 2 summarizes the complete processing chain for segmenting the grains. Figure 3 shows an example.

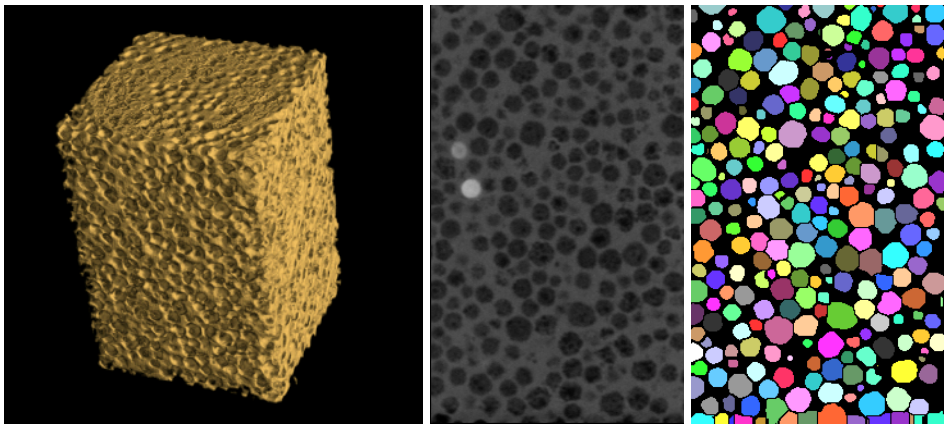

Figure 3. Syntactic foam – polymer matrix with KeraPlus grains.
Volume rendering, slice through the original reconstructed image, slice through the segmented image.
Colours are indicating the different grains.

1.2 Spatial Distribution of the Ceramic Grains

The thickness of the walls formed by the matrix between neighbouring grains is important for the mechanical properties of the composite.

In order to find the neighbours of every grain in the segmented image, the Voronoi tessellation with respect to the grains [7] is generated by growing all detected grains until they touch. All pixels closer to the current grain than to any other grain belong to its Voronoi cell. The borders of the Voronoi cells are the watersheds created by the watershed transformation with the segmented grains as starting markers [6]. Two grains are now called neighbours when their Voronoi cells are touching.

The distance between two neighbouring grains is measured using first the Euclidean distance transform on the image of one grain. This distance image is then masked by the

second grain. The minimal nonzero grey value in the resulting image is the minimal distance of the two grains and therefore the minimal wall thickness between them.

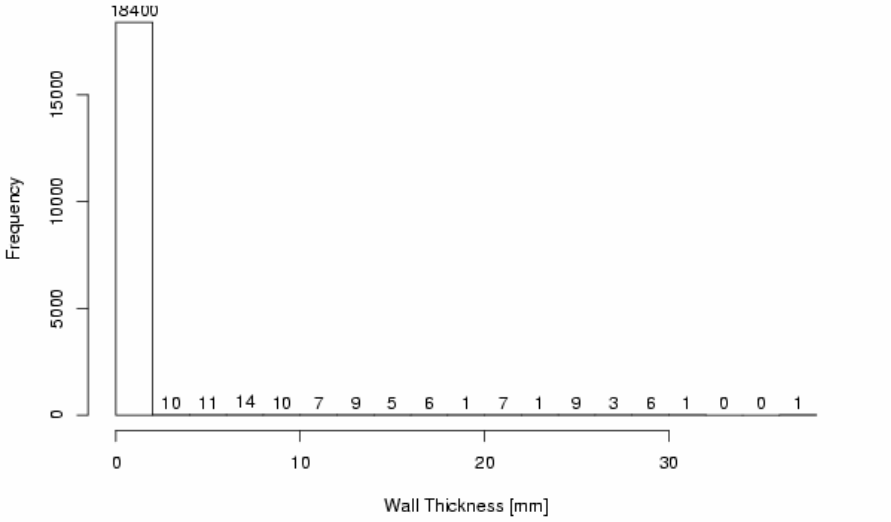

Figure 4. Histogram of the grain-to-grain distances in the syntactic polymer foam. The resolution was 0.24mm.

It turns out that nearly all walls have thicknesses near the pixel resolution, see Figure 4. That means the grains are densely packed in the foam structure.

2. Pore Structure of the Ceramic Grains

The inner structure of the ceramic grains used as inserts for the syntactic foams influences the properties of the composite. The grains should be well foamed. That is, the pore structure should be homogeneous with respect to both, volume and shape. Moreover, apertures in the outer shell can cause undesired infiltration of the grains by the matrix. Therefore, the microstructure of the grains (diameters 1–19mm) was imaged using µCT with resolutions 3–23µm.

2.1 Segmentation of the Pores

Segmentation of the pores within the ceramic grains follows the processing chain described in section 1.1 (see figure 2). Special care has to be taken due to the unexpectedly high variation of pore sizes and shapes. In particular, the walls dividing the large pores are porous, too. Moreover, some walls are broken.

Due to the high variation of pore sizes, a *height adaptive h-maxima transformation* *h*max* has to be used for the filtering step (see Figure 5). Contrary to the h-maxima transformation *h*max, *h*max* filters with respect to both, relative and absolute grey value. More precisely, following the notation in [6],

$$h\max \;\coloneqq\; R_f^{\delta}(f-h) \qquad \text{while}$$
$$h\max^* \;\coloneqq\; R_f^{\delta}(c(f-o)), \text{ with } c,o \geq 0 \text{ and } c \leq 1,$$

where R_f^δ describes reconstruction by dilation of the image *f*. Clearly, *h*max = *h*max* for *c* = 1 and *o* = *h*. Choosing $c < 1$ keeps "small" local maxima at low grey values while local maxima of the same relative height but at higher grey values are removed, see Figure 5. Additionally, a zero padding is interposed before the watershed transformation. Therewith the air/outside of the grain is marked and will be segmented as one object easy to exclude from the subsequent analysis. See Figure 6 for a sketch of the complete segmentation processing chain and Figure 7 for an example.

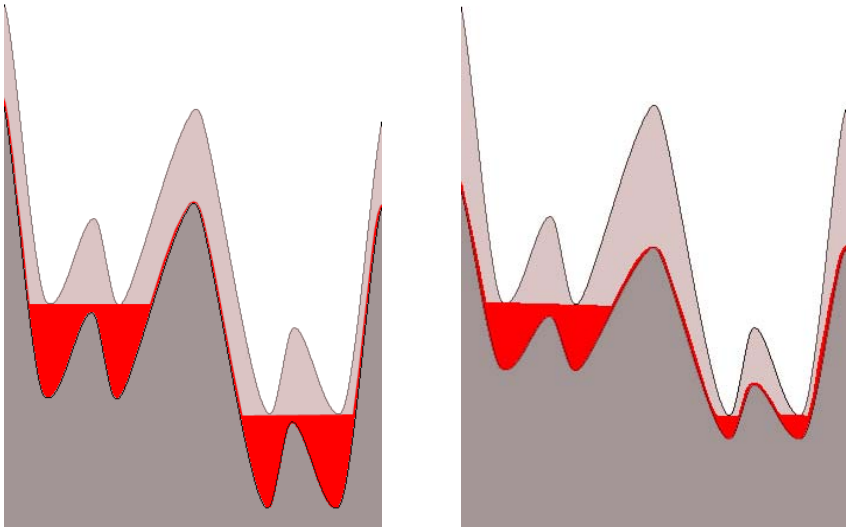

Figure 5. *Left*: Sketch of the *h*max transform.
Light grey: original image *f*, black: *f*-*h*, red: result. Local maxima with low relative height are removed.
Right: Sketch of the height adaptive *h*max* transform.
The local maximum with low relative height at high grey values is removed while the local maximum with low relative height at low grey values is kept. Thus the large pores are segmented correctly without removing the small pores within the walls.

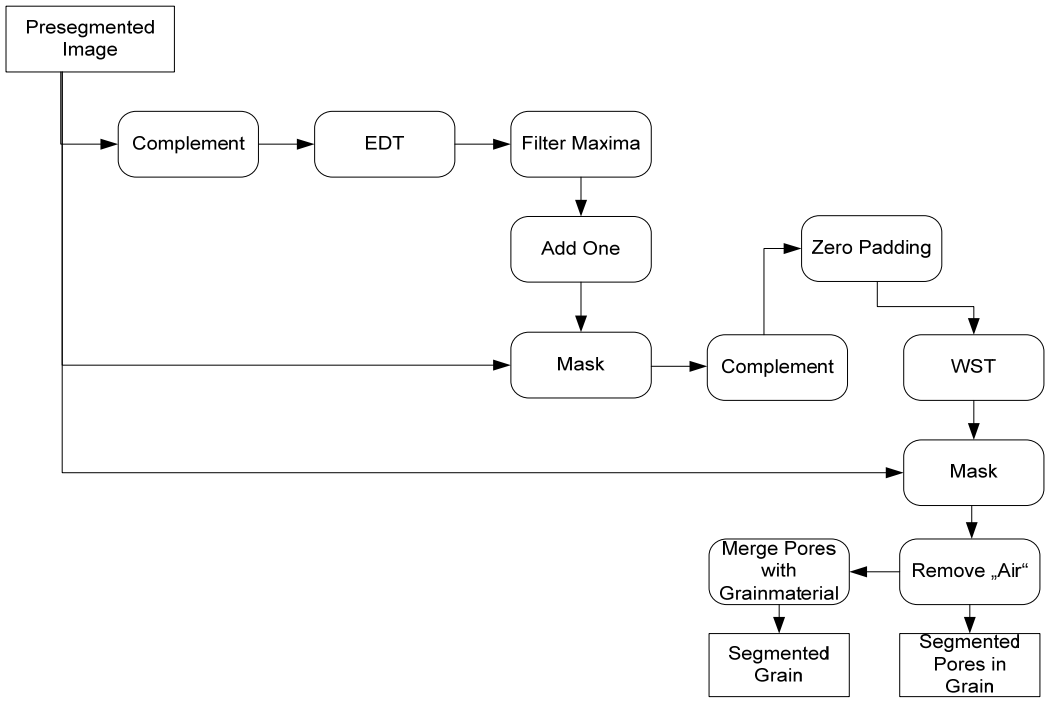

Figure 6. Processing chain for segmentation of the ceramic grain and its individual pores (EDT: Euclidean Distance Transformation, WST: Watershed Transformation).

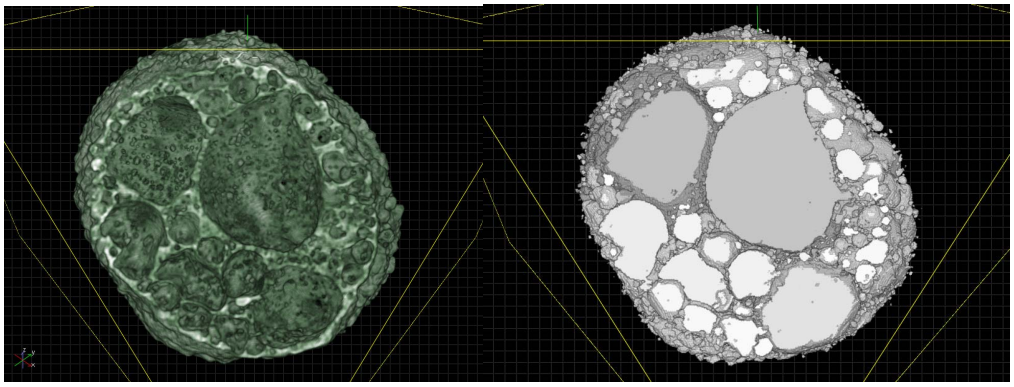

Figure 7. Volume rendering of a ceramic grain (left) and the segmented pores (right).

2.2 Geometric Characteristics

The foam structure of the ceramic grains varies strongly – there are well and badly foamed grains. An indicator for the foaming state of a grain is the shape of large pores. In badly foamed grains, the proportion of irregularly shaped grains is higher.

The shape of a 3d object can be described e.g. by its "sphericity"

$$6\sqrt{\pi}\ \frac{\text{Volume}}{(\text{Surface Area})^{\frac{3}{2}}},$$

with values in the range (0, 1], 1 being reached for the ball. Deviation from 1 measures deviation of the shape from a ball. See e.g. [8] for more information on shape factors. Figure 8 shows the histograms of the sphericity distribution of the large pores of two grains (KeraBims4–6a and KeraPlus4–8a). Clearly, in the badly foamed grain KeraBims4–6a, more irregular shapes can be observed. Volume and surface area are measured using integral-geometric methods, see [9, 10].

3. Discussion

Based on the geometric characteristics for both grains and foams, an FEM models for simulation of uniaxial compressive and tensile strength as well as elastic properties under compression load were developed, allowing to predict the mechanical properties of the composite given the mechanical properties of the components. Comparison with experimental results for syntactic foams with polymer and metal matrix shows good accordance with the simulation results [1, 11]. In both cases, strength and stiffness of the composites turned out to be stronger than the one of conventional foams with the same specific weight made of the pure matrix material.

Clearly, a considerable weight reduction for the composite can only be reached if the grains have a good pore structure and are not infiltrated by the matrix. On the other hand, slight infiltration enhances the connection between matrix and inserts and thus enhances the mechanical properties. Nevertheless, the higher the difference of the specific weights of matrix and grains, the better the mechanical properties. The influence of the spatial distribution of the grains as well as the contact between matrix and inserts are subjects of further research.

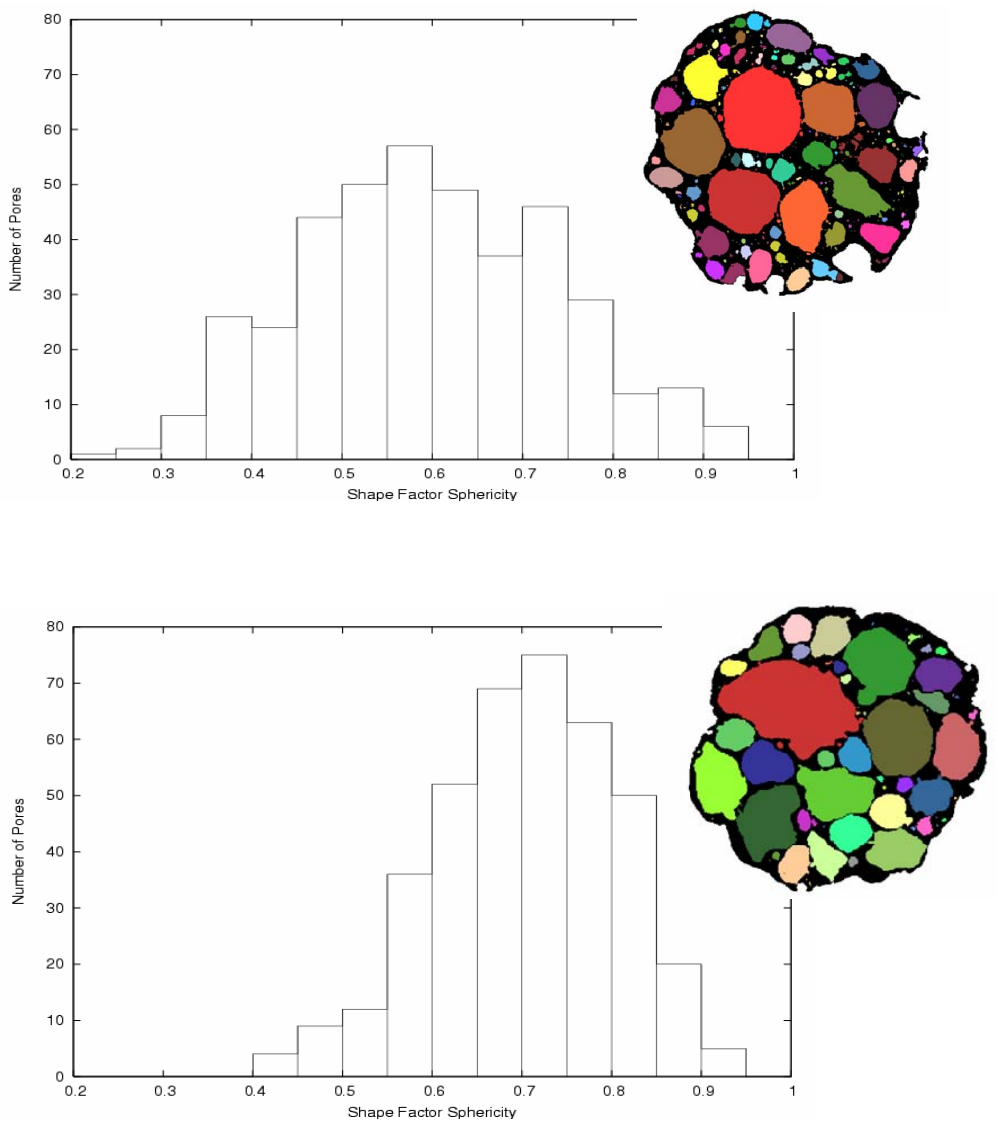

Figure 8. Histograms of the shape factor sphericity of pores. Above KeraPlus4–8a for pores with diameter larger than 0.25mm and below 0.174mm for KeraBims4–6a, respectively.
Lower bounds chosen according to the respective volumes of 142mm³ and 48mm³.
(Visualisation of slices through the segmented pore structure in the respective upper right corners.)

Acknowledgement

The presented methods and results were developed in the IMVAL project funded by the German Federal Ministry of Economics and Labour. The authors thank H. Klaus for fruitful discussions, T. Sych for the 3d visualisations, and R. Malten for help with typesetting this paper.

References

[1] H. Klaus, O. Huber, G. Kuhn. Lightweight Potential of Novel Cellular Spherical Composites, *Advanced Engineering Materials*, 7/12, 2005, S. 1117–1124.

[2] M. Godehardt. Three-dimensional images and their analysis – a new method for the characterization of open foams. *Imaging & Microscopy*, 5:32–33, 2003.

[3] M. Godehardt, K. Schladitz, and T. Sych. Analysis of volume images – a tool for understanding the microstructure of foams. In R. F. Singer, C. Körner, V. Altstädt, and H. Münstedt, editors, *Cellular Metals and Polymers*, pages 159–162, Zürich, 2005. Trans Tech Publications.

[4] O. Cuisenaire. *Distance transformations: fast algorithms and applications to medical image processing*. PhD thesis, Université catholique de Louvain, Louvain, 1999. `http://ltswww.epfl.ch/~cuisenai/papers/oc_thesis.pdf`

[5] L. Vincent and P. Soille. Watersheds in digital spaces: An efficient algorithm based on immersion simulation. *IEEE Transactions on Pattern Analysis and Machine Intelligence*, 13(6):583–598, 1991.

[6] P. Soille. *Morphological Image Analysis*. Springer-Verlag, Berlin, 1999.

[7] A. Okabe, B. Boots, K. Sugihara, and S. N. Chiu. *Spatial Tessellations – Concepts and Applications of Voronoi Diagrams*. Wiley, Chichester, second edition, 2000.

[8] K. Unverzagt, T. Sych, and J. Armbrecht. *MAVI – Modular Algorithms for Volume Images: User handbook*. Fraunhofer ITWM, Department Models and Algorithms in Image Processing, Kaiserslautern, May 2006. `http://www.itwm.fhg.de/mab/projects/MAVI/MAVI_Manual.pdf`

[9] C. Lang, J. Ohser, and R. Hilfer. On the analysis of spatial binary images. *Journal of Microscopy*, 203:303–313, 2001.

[10] J. Ohser, W. Nagel, and K. Schladitz. *Miles formulae for Boolean models observed on lattices*. In preparation, 2006.

[11] O. Huber, H. Klaus, R. Dallner, F. Bartl, K. Eigenfeld, B. Kovacs, M. Godehardt. Herstellung und Eigenschaften syntaktischer Metallschäume mit unterschiedlichen Matrix- und Füllmaterialien. Einfluss unterschiedlicher Matrix- und Füllmaterialien auf die mechanischen Eigenschaften des syntaktischen Schaums (Teil 2). *Druckguss Praxis*; März 2006, Ausgabe 2/06, S. 69–75.